Check for updates

Research Article Vol. 30, No. 15 / 18 Jul 2022 / Optics Express 27472

Optics EXPRESS

Dual-wavelength switching in InGaN quantum dot micro-cavity light-emitting diodes

YANG MEI,[1] YAN-HUI CHEN,[1] LEI-YING YING,[1] AI-QIN TIAN,[2] GUO-EN WENG,[3,4] LONG HAO,[1] JIAN-PING LIU,[2] AND BAO-PING ZHANG[1,*]

[1] *Laboratory of Micro/Nano-Optoelectronics, Department of Micro Electronic and Integrated Circuits, Xiamen University, Xiamen 361005, China*
[2] *Suzhou Institute of Nano-tech and Nano-bionics, Chinese Academy of Sciences, Suzhou 215123, China*
[3] *State Key Laboratory of Precision Spectroscopy, Department of Electronic Engineering, East China Normal University, Shanghai 200241, China*
[4] *egweng@ee.ecnu.edu.cn*
[*] *bzhang@xmu.edu.cn*

Abstract: Dual-wavelength switchable emission has been demonstrated in InGaN quantum dot (QD) micro-cavity light-emitting diodes (MCLEDs). By simply modulating the injected current levels, the output of the device can be dynamically tuned between the two distinct cavity modes at 498.5 and 541.7 nm, exhibiting deterministic mode switching in the green spectral range. Owing to the microcavity effect, high spectral purity with a narrow linewidth of 0.21 nm was obtained. According to the experimental and theoretical results, it can be concluded that the dual-wavelength switching for the investigated MCLEDs is ascribed to the broad and tunable gain of a thin InGaN QD active region, together with the mode selection and enhancement effect of the cavity. To provide additional guidelines for controllable dual-wavelength switchable operation in nitride-based light-emitting devices, detailed design and fabrication strategies are discussed. This work presents an effective method to achieve mode switching for practical applications such as multi-wavelength optical recording, frequency mixing, flip-flop and optical switches.

© 2022 Optica Publishing Group under the terms of the Optica Open Access Publishing Agreement

1. Introduction

Dual-wavelength switchable light emitters with narrow emission spectrum is a kind light source which can generate and switch light simultaneously at two distinct wavelengths, and have attracted tremendous interest in recent years due to their potential in applications including wavelength-division multiplexing (WDM) [1], dual-wavelength biological imaging [2,3], terahertz frequency generation (TFG) [4] and augmented reality (AR) systems [5]. Compared to the laser diodes (LDs), GaN-based micro-cavity light-emitting diodes (MCLEDs) provide an alternative platform to achieve the narrow emission spectrum and do not require an electronic population inversion. Through appropriate mode managements in the cavity, simultaneously emitting at several distinct wavelengths with dynamic mode tunability can be achieved [6]. Moreover, it is free of the problems in LDs such as laser speckles which needs to be eliminated when used for display applications.

The realization of large spectral range dual-wavelength emission from a microcavity device needs ingenious design for efficient mode coupling. Over the past few years, various devices and cavity structures have been developed to generate dual-wavelength emission, including two-section distributed feedback (DFB) lasers [7], mode locked nonlinearly fiber laser [8–11], quantum dot (QD) microdisk cavities [12,13], and QD photonic crystal (PC) microcavities [14]. However, the cavity design and fabrication processes are quite complicated. In contrast, a vertical-cavity configuration, such as vertical-cavity surface-emitting laser (VCSEL) and/or simplified MCLED, is more promising for precise mode modulation and wavelength control by

#464527 https://doi.org/10.1364/OE.464527
Journal © 2022 Received 19 May 2022; revised 30 Jun 2022; accepted 1 Jul 2022; published 13 Jul 2022

Optics EXPRESS

easily adjusting the cavity-length and position of active layers [15,16]. Apart from the design of cavity allowing dual-mode oscillation, the gain medium of the devices should be tunable to realize the dynamic switching between the two specific wavelengths. In 2011, Hong *et al.* reported GaN nanowire array based tunable LEDs [17]. Carriers can be controlled to be injected in different quantum wells (QWs) with different indium content locating at top and sidewall of the nanowire, so as to realize tunable characteristics of the gain medium. In 2013, Li *et al.* demonstrated the color tunable LEDs by inserting a thin layer of InGaN with low indium content between the QW layer and GaN barrier [18]. The wavelength tunability was realized by carrier redistribution in deep and shallow QWs and band filling effect. Additionally, tunable GaN-based LEDs have also been fabricated by growing semi-polar InGaN QWs with high indium content on a triangular-striped Si substrate [19], and by utilizing the Ga vacancies related donor-acceptor pair (DAP) transitions in p-GaN [20]. In these cases, however, there was no cavity configuration, so that the broad emission band was tuned continuously without the mode-switching effect.

In this study, we present InGaN QD based green MCLEDs exhibiting dual-wavelength switchable emission at two distinct wavelength of 498.5 and 541.7 nm. The mode linewidth is as narrow as 0.21 nm and the mode/background ratio is ∼18 dB, benefiting from the high quality of the micro-resonator. The dual-wavelength switchable operation is realized by the combination effect of the mode selection/enhancement of the cavity and the tunable gain of the thin QD active layer. This study provides an effective method to design and fabricate dual-wavelength switchable MCLEDs for real-world applications.

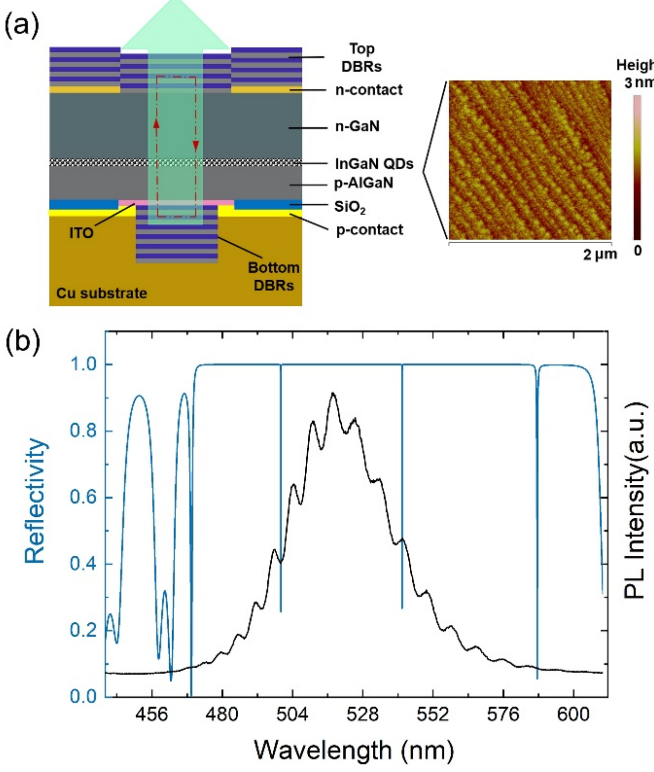

Fig. 1. (a) Cross-sectional schematic of the fabricated InGaN QD RCLED. The right insert shows a 2×2 μm^2 AFM image of the uncapped QDs. (b) Measured PL spectrum of epitaxial wafer and the calculated reflection spectrum of the cavity.

2. Materials and methods

Figure 1(a) shows the schematic illustration of the dual-wavelength switchable InGaN QD MCLED. The device is featured with dual dielectric distributed Bragg reflectors (DBRs) and a copper supporting plate. The top and bottom DBRs are 12.5 and 10 pair of SiO_2/TiO_2, respectively. The diameter of the confinement aperture is 10 µm. Detailed fabrication processes of the device are similar to our previous works [6,15,21].The epi-wafer was grown on (0001)-oriented sapphire substrate by a metal-organic chemical vapor deposition (MOCVD) system. The active region consists of two pairs of self-organized InGaN/GaN (2.5/10 nm) QDs with an average indium content of about 27%. The right insert of Fig. 1(a) shows a 2×2 μm^2 atomic force microscope (AFM) image of the uncapped InGaN QD sample, the QDs have diameters ranging from 20 to 60 nm and the estimated density is about 1.5E10 cm^{-2}. The QDs are able to relax the stress and weaken the quantum confined Stark effect (QCSE) of InGaN/GaN active region in the green spectral range [15]. The photoluminescence (PL) spectrum of the QD wafer and the calculated cavity reflection spectrum are shown in Fig. 1 (b). The PL spectrum is centered at ~ 520 nm with a full width at half maximum (FWHM) of 45 nm. The large FWHM is attributed to the inhomogeneity in QD size and indium composition. Multi-longitudinal modes can resonate simultaneously inside the cavity due to the long cavity length (~1290 nm). The broadened spontaneous emission of QDs and the multi- mode resonate cavity have laid the foundation for switchable dual-wavelength emission, which will be discussed in the following section.

3. Results and discussion

The emission of the device is collected by an objective lens and then guided to the CCD of the spectrometer through the free space optical path. Figure 2 shows the normalized electrical luminance (EL) spectra of the MCLED at different injection currents. Under the current density of 3.8 A/cm^2, a single peak at 541.7 nm first started to emerge. A second peak at 498.5 nm appeared when the current density was increased to 12.7 A/cm^2, and the intensity of the two peaks got similar at ~76 A/cm^2 with mode/background suppression ratio of 15 dB. With further increasing current, the emission is then switched to the 498.5 nm cavity mode which finally takes dominant. The mode/background suppression ratio is further increased to ~18 dB at 127 A/cm^2. The mode switching behavior here is stable and does not occur when the injected current is fixed. The device shows narrow emission peaks with a very low-level spontaneous background (SPB) emission, and the maximum output power is ~55 µW. Figure 3(a) shows the corresponding extinction ratio (defined as 10 log (I_1/I_2)) of the two emission modes (I_1 and I_2 refer to the intensity of 541.7 nm and 498.5 nm mode, respectively). The extinction ratio changed from 7.5 to −6 dB with the increase of current density, demonstrating the switchable property of our QD MCLEDs. Figure 3(b) shows the high-resolution spectra of the two emission modes. The linewidths are 0.21 nm and 0.45 nm, inducing cavity quality factor Q of 2579 and 1107 for the two cavity modes, respectively. The smaller Q factor of the mode with higher energy at 498.5 nm can be induced by the increased optical absorption of the active region. Both the 541.7 nm and 498.5 nm mode are featured with multi-peak structure, and these peaks are different order lateral confined modes because there is lateral optical boundary in the device formed by the SiO_2 confinement aperture. The current-voltage (I-V) as well as the emission profile of the device are given in Fig. 4. The turn on voltage is ~3.0 V, and the reverse leakage current under a bias voltage of -5 V is less than 2 nA, as shown in the inset of Fig. 4. The insets of Fig. 4 also show the near field emission pattern of an operating device, which shows bright emission in green.

To further investigate the mechanism of tunable emission, the integrated intensity ratio in 541.7 and 498.5 nm emission modes, as well as the SPBs versus injected current density is plotted in Fig. 5(a). The evolution of each channel at different current density can be generally divided into three stages. At stage I with low injection level from 3 to 20 A/cm^2, the broadband SPB

Optics EXPRESS

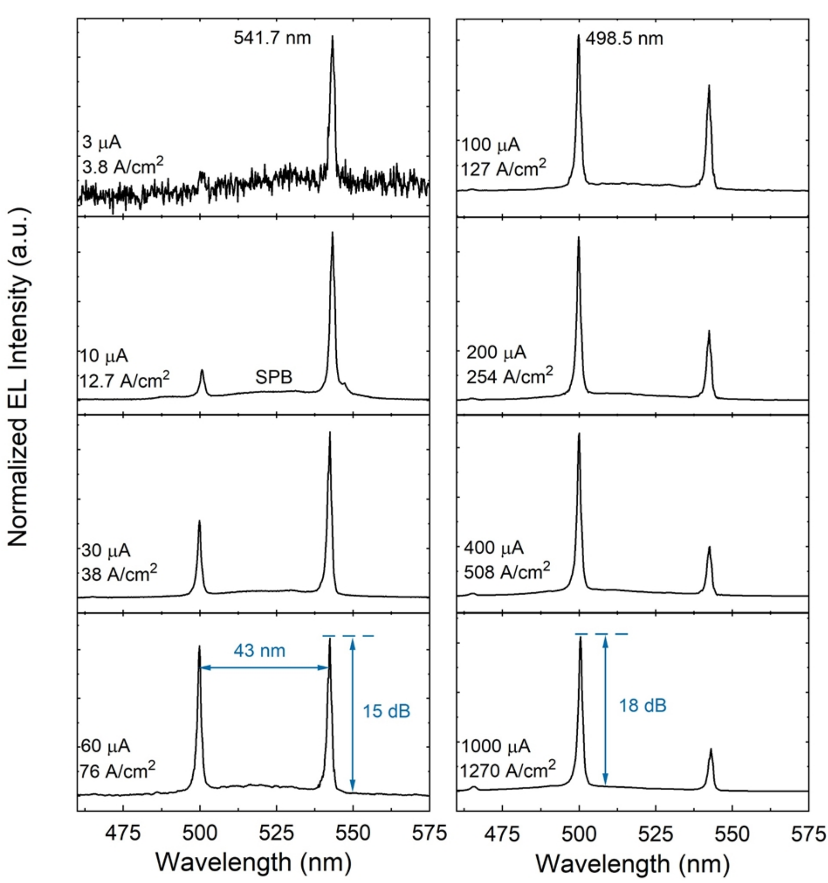

Fig. 2. Measured EL spectra at different current density of the dual-wavelength switchable MC light emitter.

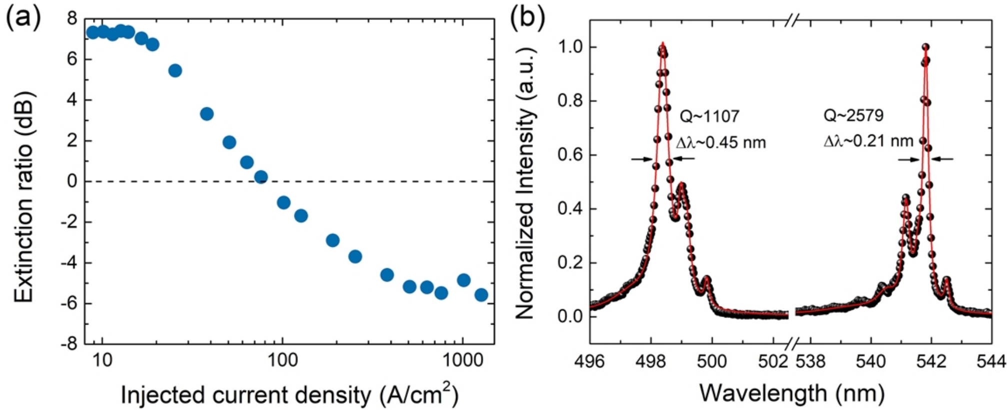

Fig. 3. (a) Extinction ratio of the two distinct modes. (b) High resolution spectra of the 498.5 and 541.7 nm cavity modes.

Optics EXPRESS

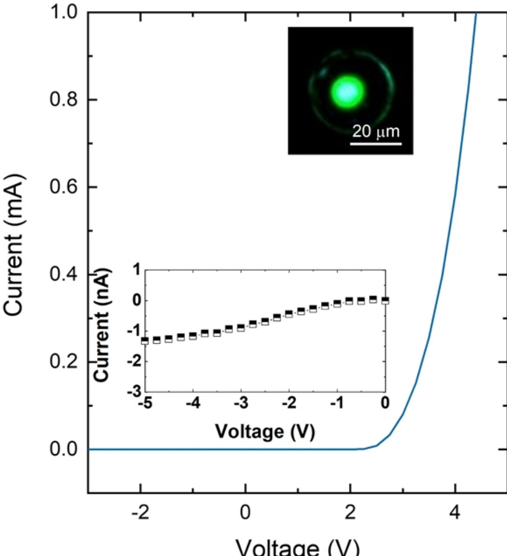

Fig. 4. IV curve of the green RCLED. The insets show the reverse biased IV curve, as well as the photos of an operating device.

emission from 480 to 560 nm takes dominant and decreases with increasing current. On the other hand, component of the 541.7 nm cavity mode increases rapidly and reaches the maximum at around 20 A/cm^2. The component of the 498.5 nm cavity mode is weak and keeps almost constant during this stage due to the small material gain at this wavelength under low injection level. This indicates that SPB is suppressed and the emission of carriers is mainly channeled to the 541.7 nm cavity mode during this stage. At stage II from 20 to 80 A/cm^2, material gain is tuned and induce the rapid increase at shorter wavelengths, leading to the mode change from the 541.7 nm to the 498.5 nm cavity mode. Meanwhile, the ratio of SPB keeps nearly constant in this stage. At stage III, the 498.5 nm cavity mode finally takes dominant, and the 541.7 nm mode and SPB are further suppressed. To more clearly illustrate the tunable characteristics of the InGaN QD MCLED, the Commission International de I'Elairage (CIE) chromaticity coordinates at various currents are shown in Fig. 5(b). As the current density increases from 3 to 1000 μA, the CIE coordinates move from (0.26, 0.74) to (0.12, 0.43), corresponding to the color of yellow-green to cyan. This relationship between CIE coordinate and injection current demonstrates the current-driven color-tunable characteristic, which can be useful for the applications including full color projection and mood lighting.

The dual wavelength switchable operation in this study is mainly based on two factors, one comes from the cavity effect, in both mode selection and gain enhancement, the other is the tunable material gain of InGaN QDs with injection current. In a cavity, only the emission with wavelengths coupled with the cavity modes are allowed, so as to realize the narrow emission peaks (mode selection role). In addition, the mode intensity strongly depends on the magnitude of coupling condition between the mode standing wave field and gain medium, and can be reflected by the gain enhancement factor Γ_r defined by [6]

$$\Gamma_{\mathrm{r}} = \frac{L}{d}\frac{\int_d |E(z)|^2 \mathrm{d}z}{\int_L |E(z)|^2 \mathrm{d}z} \tag{1}$$

Optics EXPRESS

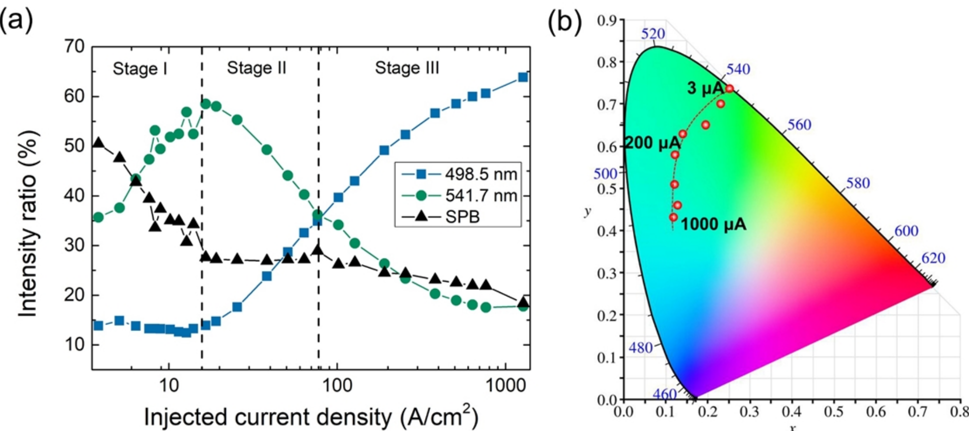

Fig. 5. (a) Intensity ratio in 498.5 nm/503 nm/SPB channels versus injection current density. (b) CIE chromaticity coordinates at various current density.

where L, d, $E(z)$ are the cavity length, thickness of the active region and optical field, respectively. The well coupled cavity modes (active region overlaps with the antinode of the mode standing-wave pattern) could be boost due to the enhanced interaction between electrons and photons, in other words, large Γ_r value. In contrast, the weak coupled cavity modes (active region overlaps with the node of the mode standing-wave pattern) is suppressed, in other words, small Γ_r value [6]. The gain enhancement caused by cavity effect also depends greatly on the thickness of the active layer. Figure 6 shows the calculated Γ_r for the resonate modes in a cavity with different active layer thicknesses, in which the black solid curve represents the Γ_r of a well coupled mode and the red dashed curve represents the weak coupled mode, respectively. For a very thin active layer, the Γ_r varies much between 0 and 2 depending on the coupling condition between the mode profile and active region. Such a large difference in Γ_r will modulate the emission rate of the cavity modes with different coupling condition, inducing the enhancement or suppression effect. However, with increasing active layer thickness, the difference of Γ_r between cavity modes with different coupling condition is gradually decreased. When the active layer thickness is increased to $\lambda/4n_c$, Γ_r for cavity modes with different coupling condition is equal to 1. Under this condition, there is no difference between "well coupled" and "weak coupled". With further increasing active layer thickness, the difference between the Γ_r of the weak and well coupled modes is also limited in a small range. Therefore, a thin active layer is essential for switchable multi-wavelength devices to select and enhance particular distinct peaks among multi-resonate modes by utilizing the cavity effect.

To explain more clearly the design principle and the mechanism of the dual-wavelength switchable emission in a large spectral range, a half cavity (without top DBR) device with a longer cavity (~4 μm) was fabricated, and Fig. 7(a) shows the normalized emission spectra under different currents. Longer cavity allows more longitudinal modes to simultaneously resonate, enabling us to investigate and compare the modulation effect of Γ_r on cavity modes with different coupling conditions. The multi-longitudinal resonate modes can be clearly observed in the spectra due to the interference between bottom DBR and top GaN/air interface. The spectra show a blue shift with increasing current. The longer wavelength part (~540-570 nm) takes dominant under low injection, while the shorter wavelength part (480-510 nm) is stronger under high injection. However, the spectra around 510-535 nm is always suppressed during evolution and a gap is formed. The blue shift can be explained by the combined effect of band filling and size effect of InGaN QDs. QDs with smaller size can generate light with shorter wavelength,

Optics EXPRESS

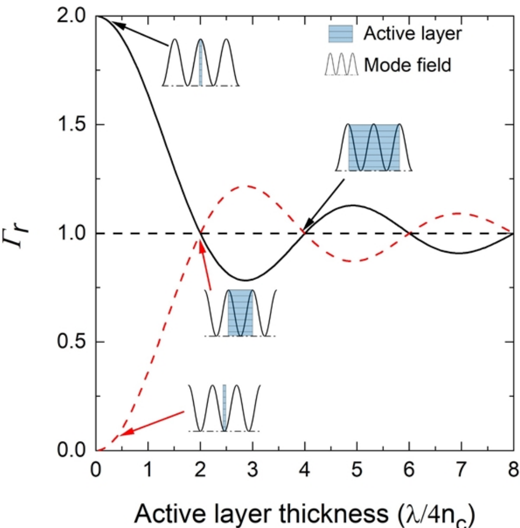

Fig. 6. Calculated Γ_r as a function of active layer thickness for the well and weak coupled modes. The insets show the coupling between active layer and mode field under several particular conditions.

while the QD size bigger the emission wavelength longer [12]. Usually the emission of bigger QDs is stronger under low injection level because of their larger carrier capture cross section. The emission of small QDs will take dominant under high injection level due to their higher emission rate [12]. The mode enhancement and suppression appeared here is caused by the different Γ_r of each modes. For a given cavity, Γ_r as a function of resonating wavelength can be calculated by [22]:

$$\Gamma_r = 1 + \frac{2r_2}{\beta d(1 + r_2^2)}[\sin \beta d \cos(2\beta L_2 + \beta d + \psi_2)] \quad (2)$$

where β is the propagation constant β=2πn/λ (λ is the vacuum wavelength and n is the refractive index), r_2 is the reflectance of bottom DBR, L_2 is the separation between the active layer and the bottom DBRs, ψ_2 is the reflection phase shift of the bottom DBR. The calculated results for the cavity in this study is illustrated in Fig. 7(b). Since the InGaN QD active region is very thin of ~25 nm (~0.12 λ), the coupling condition of mode field with the active layer can be very different among all the cavity modes with different wavelengths. Here, we define the wavelength range where Γ_r larger than 1 as the enhanced region and smaller than 1 as the suppressed region. Distribution of these regions match well with the corresponding part of the spectra in Fig. 7(a), indicating the selection and enhancement of particular emission modes caused by cavity effect. Figure 7(b) also shows the EL spectrum of the dual wavelength switchable device under 60 μA from Fig. 2, and both cavity modes are located in the enhanced region. Although the mode wavelengths are slightly deviated from the center of the enhanced region, this can be solved by further optimization of cavity length, and dual wavelength switchable devices with larger switching wavelength and extinction ratio can be expected. The device exhibits only two modes in the enhanced gain spectral region in this study. But according to our previous work, even if other cavity modes appeared in the suppressed region, the mode intensity can be well suppressed, guaranteeing the dual wavelength switchable operation [6].

The dual wavelength switchable operation in this study is realized by a thin QD active region with tunable gain and mode selection of cavity effect. For general device fabrication, we give the

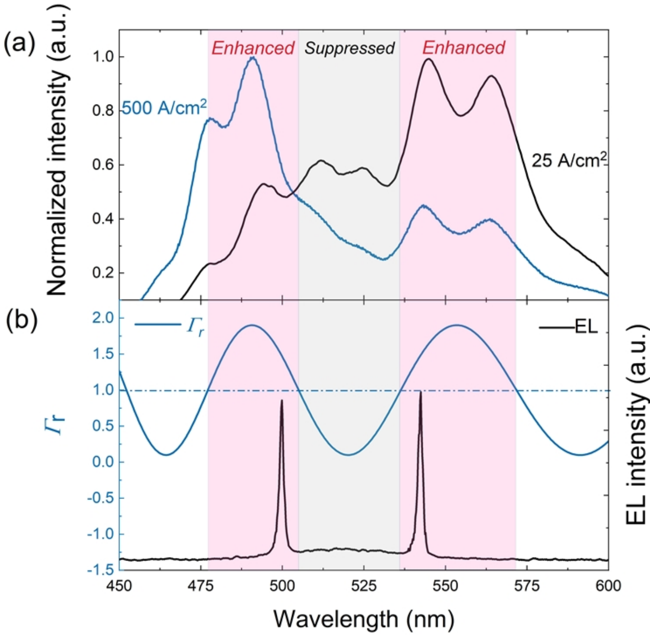

Fig. 7. (a) Normalized EL spectra of a half-cavity device under different current. (b) EL spectrum of the dual wavelength switchable device and the calculated Γ_r as a function of resonating wavelength.

following detailed design strategies and implementation methods which can provide a guideline to realize robust dual or multi-wavelength switchable and tunable devices. First, according to the target switching wavelengths (e.g., λ1 and λ3 in Fig. 8), the cavity length as well as the reflection band of the DBR can be determined, because the resonating wavelength can be derived from the cavity length and phase condition of DBR. The control of cavity length during device fabrication can be realized by either CMP process for dual dielectric DBR configuration, or epitaxial growth of cavity layers for hybrid DBR schemes. Once the DBR and cavity length are fixed, the optical fields of the cavity modes at the target resonating wavelengths can be calculated through the transfer matrix method (TMM), as schematically shown in Fig. 8(a). Second, the active layer should be thin enough and locates near the antinode of standing wave pattern of both mode λ_1 and λ_3 to ensure strong mode coupling. The position of this thin active layer can be controlled during the MOCVD growth of the epitaxial wafer. Here, a third mode with bad coupling condition (λ_2) was also plotted in Fig. 8(a) to schematically show the suppression effect of the bad coupled modes. But one doesn't need to design such modes intentionally in real device fabrication. The tunable gain of the active region is also very important for realization of tunable/switchable operation and should cover modes λ_1 and λ_3, as illustrated in Fig. 8(b) and 8(c). QD layers with varying dot size was used in this study to obtain the tunable material gain. Nevertheless, large wavelength scale tunable emission has also been achieved by InGaN QWs with special designs [18–20]. Based on the careful spectral alignment between the resonating wavelength and gain peaks, and the spatial alignment between active layer and optical field, efficient dual or multi-wavelength switchable emission can be expected, and the bad coupled modes can be well suppressed, as illustrated in Fig. 8(d).

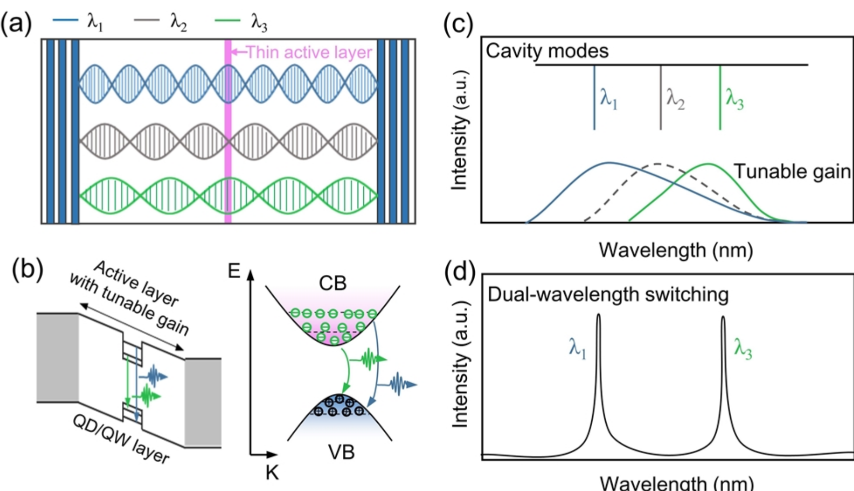

Fig. 8. (a) Schematic structure and mode profile of dual wavelength switchable microcavity device. A thin active layers is placed at the antinode of both resonating modes. (b) Schematic structure of the active region with tunable gain characteristics. (c, d) Spectral alignment between the tunable gain peaks and the resonating modes in the cavity and the inducing operation of dual-wavelength switching.

4. Conclusion

In summary, dual-wavelength switchable emission in large spectral range with narrow emission spectrum was demonstrated in an InGaN QD based MCLED. The device output spectrum can be switched between the 498.5nm and 541.7 nm cavity mode, with spontaneous emission background perfectly suppressed. The switching wavelength range is as large as 43 nm, and the linewidth of the emission modes is as narrow as 0.21 nm. The dual-wavelength switchable emission is realized by the combination of a thin active layer with tunable gain spectrum and a multi-modes resonated cavity. The difference in Γ_r of the cavity modes leads to mode selection and enhancing effect, and finally inducing the dual-wavelength switchable emission. This work has proposed an effective design principle for dual-wavelength switchable MCLEDs for specific applications.

Funding. National Key Research and Development Program of China (2017YFE0131500); National Natural Science Foundation of China (61704055, 62104204, U21A20493).

Acknowledgments. This work was supported by the National Key Research and Development Program of China and the National Natural Science Foundation of China.

Disclosures. There is no conflict of interest.

Data availability. Data underlying the results presented in this paper are not publicly available at this time but may be obtained from the authors upon reasonable request.

References

1. P. Winzer, "Making spatial multiplexing a reality," Nat. Photonics **8**(5), 345–348 (2014).
2. M. Trieschmann, B. Heimes, H. Hense, and D. Pauleikhoff, "Macular pigment optical density measurement in autofluorescence imaging: comparison of one-and two-wavelength methods," Graefe's Arch. Clin. Exp. Ophthalmol. **244**(12), 1565–1574 (2006).
3. M. Wu, K. Jansen, A. F. van der Steen, and G. van Soest, "Specific imaging of atherosclerotic plaque lipids with two-wavelength intravascular photoacoustics," Biomed. Opt. Express **6**(9), 3276–3286 (2015).
4. L. Sánchez-García, M. O. Ramírez, R. M. Solé, J. J. Carvajal, F. Díaz, and L. E. Bausá, "Plasmon-induced dual-wavelength operation in a Yb 3 + laser," Light: Sci. Appl. **8**(1), 14 (2019).

Optics EXPRESS

5. K. Hong, J. Yeom, C. Jang, J. Hong, and B. Lee, "Full-color lens-array holographic optical element for three-dimensional optical see-through augmented reality," Opt. Lett. **39**(1), 127–130 (2014).
6. Y. Mei, R.-B. Xu, G.-E. Weng, H. Xu, L.-Y. Ying, Z.-W. Zheng, H. Long, B.-P. Zhang, W. Hofmann, and J.-P. Liu, "Tunable InGaN quantum dot microcavity light emitters with 129 nm tuning range from yellow-green to violet," Appl. Phys. Lett. **111**(12), 121107 (2017).
7. T. G. Folland and S. J. I. P. T. L. Chakraborty, "Dual-Frequency Defect-Mode Lasing in Aperiodic Distributed Feedback Cavities," IEEE Photonics Technol. Lett. **28**(15), 1617–1620 (2016).
8. J. S. Liu, X. H. Li, Y. X. Guo, A. Qyyum, Z. J. Shi, T. C. Feng, Y. Zhang, C. X. Jiang, and X. F. Liu, "SnSe2 Nanosheets for Subpicosecond Harmonic Mode-Locked Pulse Generation," Small **15**(38), 1902811 (2019).
9. X. Wang, Y. J. Zhu, C. Jiang, Y. X. Guo, X. T. Ge, H. M. Chen, J. Q. Ning, C. C. Zheng, Y. Peng, X. H. Li, and Z. Y. Zhang, "InAs/GaAs quantum dot semiconductor saturable absorber for controllable dual-wavelength passively Q-switched fiber laser," Opt. Express **27**(15), 20649–20658 (2019).
10. Y. Zhao, P. Guo, X. Li, and Z. Jin, "Ultrafast photonics application of graphdiyne in the optical communication region," Carbon **149**, 336–341 (2019).
11. S. Lv, X. Liu, X. Li, W. Luo, W. Xu, Z. Shi, Y. Ren, C. Zhang, and K. Zhang, "Electrochemical Peeling Few-Layer SnSe2 for High-Performance Ultrafast Photonics," ACS Appl. Mater. Interfaces **12**(38), 43049–43057 (2020).
12. A. Woolf, T. Puchtler, I. Aharonovich, T. Zhu, N. Niu, D. Wang, R. Oliver, and E. L. Hu, "Distinctive signature of indium gallium nitride quantum dot lasing in microdisk cavities," Proc. Natl. Acad. Sci. **111**(39), 14042–14046 (2014).
13. Y. Mei, M. Xie, H. Long, L. Ying, and B. Zhang, "Low Threshold GaN-Based Microdisk Lasers on Silicon With High Q Factor," J. Lightwave Technol. **40**(9), 2952–2958 (2022).
14. S. Chakravarty, P. Bhattacharya, S. Chakrabarti, and Z. J. O. L. Mi, "Multiwavelength ultralow-threshold lasing in quantum dot photonic crystal microcavities," Opt. Lett. **32**(10), 1296–1298 (2007).
15. Y. Mei, G.-E. Weng, B.-P. Zhang, J.-P. Liu, W. Hofmann, L.-Y. Ying, J.-Y. Zhang, Z.-C. Li, H. Yang, and H.-C. Kuo, "Quantum dot vertical-cavity surface-emitting lasers covering the green gap," Light: Sci. Appl. **6**, e16199 (2017).
16. Y. Mei, T.-R. Yang, W. Ou, Z.-M. Zheng, H. Long, L.-Y. Ying, and B.-P. J. F. R. Zhang, "Low-threshold wavelength-tunable ultraviolet vertical-cavity surface-emitting lasers from 376 to 409 nm," Fundam. Res. **1**(6), 684–690 (2021).
17. Y. J. Hong, C. H. Lee, A. Yoon, M. Kim, H. K. Seong, H. J. Chung, C. Sone, Y. J. Park, and G. C. Yi, "Visible-color-tunable light-emitting diodes," Adv. Mater. **23**(29), 3284–3288 (2011).
18. H. Li, P. Li, J. Kang, Z. Li, Z. Li, J. Li, X. Yi, and G. Wang, "Phosphor-Free, Color-Tunable Monolithic InGaN Light-Emitting Diodes," Appl. Phys. Express **6**(10), 102103 (2013).
19. Q. Wang, G. Yuan, W. Liu, S. Zhao, Z. Liu, Y. Chen, J. Wang, and J. Li, "Semipolar (1101) InGaN/GaN red–amber–yellow light-emitting diodes on triangular-striped Si (100) substrate," J. Mater. Sci. **54**(10), 7780–7788 (2019).
20. Y. Huang, F. Yun, Y. Li, W. Ding, Y. Wang, H. Wang, W. Zhang, Y. Zhang, M. Guo, S. Liu, and X. Hou, "Defect-induced color-tunable monolithic GaN-based light-emitting diodes," Appl. Phys. Express **7**, 1 (2014).
21. Y. Mei, Y.-H. Chen, L.-Y. Ying, Z.-W. Zheng, H. Long, and B.-P. Zhang, "High Q factor Electrically Injected Green Micro Cavity," J. Lightwave Technol. **39**(9), 2895–2901 (2021).
22. M. S. Ünlü and S. Strite, "Resonant cavity enhanced photonic devices," J. Appl. Phys. **78**(2), 607–639 (1995).

117.28.251.250 on 2022-07-13 20:54:01